Proceedings of the 2012 IEEE 12th International Conference on Bioinformatics
& Bioengineering (BIBE), Larnaca, Cyprus, 11-13 November 2012

Application of fast segmentation method for knee contour delineation

Antonio Pinti[1,5]
[1] ENSIAME – UVHC, Université de Valenciennes, 59300 Valenciennes, France
antonio.pinti@univ-valenciennes.fr

Raphael Coursier[2]
[2] Groupe Hospitalier de l'Institut Catholique de Lille, 59462 Lomme, France
coursier.raphael@ghicl.net

Eric Watelain[3,4]
[3] LAMIH – UMR 8201 CNRS, Université de Valenciennes, 59300 Valenciennes, France
[4]Handibio, EA 4322, Université Du Sud Toulon Var, BP 20132 8395 La Garde Cedex, France
eric.watelain@univ-valenciennes.fr

Hechmi Toumi[5]
[5] EA 4708, I3MTO, CHRO 1, rue Porte Madeleine, 45032 Orléans, France
hechmi.toumi@univ-orleans.fr

Abstract — We present a fully automatic model based system for segmenting bone MR images of the knee. The segmentation method is based on a fast Active Appearance Models (AAM) based on canonical correlation analysis algorithm (CCA-AAM) where the dependency between texture residuals and model parameters are estimated in fast manner. The model is built from manually segmented examples from the knee images. The model has been applied to some challenging knee MR images. Experiments show that CCA-AAMs based segmentation, while requiring similar implementation effort, consistently outperform segmentation model based traditional AAM. Finally, we show results on knee image to illustrate the performance that are possible.

Keywords— AAM, CCA, knee, segmentation.

I. INTRODUCTION

Fully automated segmentation of bone and cartilage could be massively beneficial in clinical trials and in the orthopaedic industry. Quantitative image analysis of cartilage from knee MRI is a well established method but its use in medium to large scale clinical studies has been hindered by the need for manual segmentation of the cartilage. Manual segmentation has been shown to be sufficiently sensitive to detect change [5], but is labour intensive, taking up to several hours per image, which impacts on the size of clinical trials and cost. Small trials are less well powered and less likely to detect a change. In orthopaedics, detailed information from MR and CT can be used to plan for the best positioning of surgical cuts, allow intra-operative plan registration and inform prosthesis design. We have developed a statistical model-based segmentation method for the analysis of bone, cartilage and other soft tissues to meet these needs. The model is based on the Active Appearance Models AAM of Cootes et al [7], in which the statistics of shape and image information are calculated from a training set of images and used to match to new images.

The goal of AAM is to find the model parameters that generate a synthetic image as close as possible to a given input image and to use the resulting AAM parameters for interpretation [1,5]. Matching the model and target image is treated as an optimization problem, i.e., the problem of minimizing the texture residual with regard to model parameters. Provided that the model is roughly aligned with the target image, the relation of texture residuals and parameter updates can be modeled as a class of tissue [1,5]. In the traditional AAM [5], the mapping from error images to AAM parameters is modeled by a linear regression approach such as linear least-squares estimates. Herein, [5], the regression estimates were replaced by a simplified Gauss-Newton procedure, where the Jacobian matrix is evaluated only once by numerical differentiation from training data. Throughout this paper, we will refer to this as standard approach. Both approaches are similar in the sense that they assume that the error surface can be approximated well by a quadratic function. The main advantage of the latter approach [7] is that, during training, not all different images have to used. Various approaches to increase convergence accuracy of the AAM have been proposed in [1]. Shape AAM [3] update only pose and shape parameters during segmentation, while gray-level parameters are computed directly from the image sample. This allows the AAM to converge faster but the failure rate increases. Direct appearance models [7] predict shape parameters directly from texture. The convergence speed of AAM for tracking applications is investigated in [6]. These modifications of the AAM improve the convergence speed and the quality of the results by reducing either the number of parameters that are to be optimized or the computational cost.

II. SEGMENTATION METHOD

An appearance model is a statistical model of the shape of a structure and associated imaging information. It is useful to process the imaging information further to obtain feature response images such as gradients, corners and other points of interest [1].

A. Active Appearance Models

The concept of AAM as described in [5] is based on the idea of combining both shape and texture information of the objects to be modeled. First, the shape vectors $\mathbf{x}^i = \left(x_1^i,\ldots,x_n^i,y_1^i,\ldots,y_n^i\right)^T$ $, i=1,\ldots,N$ of the N training images are aligned using Procrustes analysis. The images are warped to the mean shape $\overline{\mathbf{x}}$ and normalized, yielding the texture vectors $\mathbf{g}^i$. By applying Principal Component Analysis (PCA) to the normalized data, linear models are obtained for both shape:

$$\mathbf{x} = \overline{\mathbf{x}} + \mathbf{P}_s\mathbf{b}_s \qquad (1)$$

and texture:

$$\mathbf{g} = \mathbf{g} + \mathbf{P}_g\mathbf{b}_g \qquad (2)$$

Where $\mathbf{x}$; $\mathbf{g}$ are the mean vectors, $\mathbf{P}_s$, $\mathbf{P}_g$ are sets of orthogonal modes of variation (the eigenvectors resulting from Principal Component Analysis) and $\mathbf{b}_s$, $\mathbf{b}_g$ are sets of model parameters. A given object can thus be described by $\mathbf{b}_s$ and $\mathbf{b}_g$. As $\mathbf{P}_s$; $\mathbf{P}_g$ may still be correlated, PCA is applied once more using the following concatenated vector:

$$\mathbf{b} = \begin{pmatrix} \mathbf{W}_s\mathbf{b}_s \\ \mathbf{b}_g \end{pmatrix} = \begin{pmatrix} \mathbf{W}_s\mathbf{P}_s^T(\mathbf{x}-\overline{\mathbf{x}}) \\ \mathbf{P}_g^T(\mathbf{g}-\overline{\mathbf{g}}) \end{pmatrix} \qquad (3)$$

where $\mathbf{W}_s$ is a diagonal scaling matrix derived from the value ranges of the eigenvalues of the shape and texture eigenspaces. This yields the final combined linear model $\mathbf{b} = \mathbf{P}_c\mathbf{c}$, where $\mathbf{P}_c = \left(\mathbf{P}_{cs}^T + \mathbf{P}_{cg}^T\right)^T$. Shape free images and the corresponding shapes defining the deformation of the texture can be expressed directly using $\mathbf{c}$ by:

$$\mathbf{x} = \overline{\mathbf{x}} + \mathbf{P}_s\mathbf{W}_s^{-1}\mathbf{P}_{cs}\mathbf{c} \qquad (4)$$

and the texture by:

$$\mathbf{g} = \overline{\mathbf{g}} + \mathbf{P}_g\mathbf{P}_{cg}\mathbf{c} \qquad (5)$$

To enable the model to deal with rotation, scaling s, and translation the additional model parameters $\mathbf{t}$, capturing scaling and rotation and $\mathbf{u}$, modeling image contrast and brightness, are introduced. The resulting AAM model represents shape and texture variation of image content utilizing a single parameter vector $\boldsymbol{p} = \left(\boldsymbol{c}^T \middle| \boldsymbol{t}^T \middle| \boldsymbol{u}^T\right) \in \boldsymbol{R}^q$.

B. FAST APPEARANCE MODELS

We train the AAM where model parameters $\mathbf{p}$ generate learned images $I_m(\mathbf{p})$, the AAM for an optimal match minimizes the difference between a given image I_m and the learned image $I_m(\mathbf{p})$. The AAM for the model parameters p can be guided by using prior knowledge about how the different images correlate with the parameter displacements. This prior knowledge is obtained during the training step. During each search step, the current image residual between the texture model $\mathbf{g}_m(\mathbf{p})$ and the sampled image patch $\mathbf{g}_s(\mathbf{p})$ is computed as:

$$r(\mathbf{p}) = \mathbf{g}_s(\mathbf{p}) - \mathbf{g}_m(\mathbf{p}) \qquad (6)$$

The search procedure aims at minimizing the sum of square (pixel) error:

$$er(\mathbf{p}) = \frac{1}{2}\mathbf{r}(\mathbf{p})^T\mathbf{r}(\mathbf{p}) \qquad (7)$$

Following the standard Gauss-Newton optimization method one approximates (linearizes) using the first-order Taylor expansion:

$$\frac{\Delta\mathbf{r}}{\Delta\mathbf{p}} = \frac{\mathbf{r}(\mathbf{p}+\Delta\mathbf{p}) - \mathbf{r}(\mathbf{p})}{\Delta\mathbf{p}} \qquad (8)$$

The derivative of with regard to $\mathbf{p}$ and setting it to zero gives:

$$\Delta\mathbf{p} = -\mathbf{R}\mathbf{r}(\mathbf{p}) \qquad (9)$$

Where

$$\mathbf{R} = \left(\frac{\Delta\mathbf{r}^T}{\Delta\mathbf{p}}\frac{\Delta\mathbf{r}}{\Delta\mathbf{p}}\right)^{-1}\frac{\Delta\mathbf{r}^T}{\Delta\mathbf{p}} \qquad (10)$$

Where $\frac{\Delta\mathbf{r}}{\Delta\mathbf{p}}$ is calculated during training using numeric differentiation.

During training, each parameter is displaced from its optimal value in h steps from -1 to +1 standard deviations, and a weighted average of the resulting difference images over the training set. Each iteration updates the AAM parameters using:

$$\begin{aligned} \mathbf{p}_{estimated} &= \mathbf{p} + s\Delta\mathbf{p} \\ \Delta\mathbf{p} &= -\mathbf{R}\mathbf{r} \end{aligned} \qquad (11)$$

At each of these scaling steps, the image patch is compared to the learned image $I_m(\mathbf{p})$ [7].

C. CANONICAL CORRELATION ANALYSIS

Canonical Correlation Analysis is a very powerful tool that is especially well suited for relating two sets of measurements. Given two zero-mean random vector data sets $\boldsymbol{x} \in \boldsymbol{R}^p$ and $\boldsymbol{y} \in \boldsymbol{R}^q$, CCA finds pairs of directions $\mathbf{w}_x$ and $\mathbf{w}_y$ that maximize the correlation between the projections $x = \mathbf{w}_x^T\mathbf{x}$ and $y = \mathbf{w}_y^T\mathbf{y}$. More formally, the directions can be found as maxima of the function:

$$\rho = \frac{E(xy)}{\sqrt{E(x^2)E(y^2)}} = \frac{\mathbf{w}_x^T \mathbf{C}_{xy} \mathbf{w}_y}{\sqrt{\mathbf{w}_x^T \mathbf{C}_{xx} \mathbf{w}_x \mathbf{w}_y^T \mathbf{C}_{yy} \mathbf{w}_y}} \quad (12)$$

where $C_{xx} \in R^{p \times p}$ and $C_{yy} \in R^{q \times q}$ are the within-set covariance matrices of x and y (in the context of CCA, the projections x and y are also referred to as canonical variates, while $C_{xy} \in R^{p \times q}$ denotes their between-set covariance matrix. The factor pairs $\mathbf{w}^i$ can be obtained as eigenvectors of a generalized eigenproblem [20]:

$$\mathbf{w}^i = \left(\mathbf{w}_x^{iT}, \mathbf{w}_y^{iT}\right)^T = \begin{cases} \arg\max\limits_{\mathbf{w}_x^i, \mathbf{w}_y^i} \{\rho\} \\ \rho\left(\mathbf{w}_x^i, \mathbf{w}_y^j\right) = \rho\left(\mathbf{w}_x^j, \mathbf{w}_y^i\right) = 0, j = 0, \ldots, i-1 \end{cases} \quad (13)$$

The extremum values $\rho\left(\mathbf{w}^i\right)$, which are referred to as canonical correlations, are obtained as the corresponding eigenvalues.

III. FAST CCA-AAM

In the standard AAM search algorithm, a linear function (see (3)) is used to map texture residuals $\mathbf{r}(\mathbf{p})$ to corresponding parameter displacements $\Delta\mathbf{r}(\mathbf{p})$. In The AAM algorithm, the linear features of $\mathbf{r}(\mathbf{p})$ are extracted using the CCA of $\mathbf{r}(\mathbf{p})$ and $\mathbf{p}$.

A. CCA-AAM Training

For each training image, we generate a set of synthetic images by perturbing the optimal AAM match, i.e., $\mathbf{r}(\mathbf{p}_o + \Delta\mathbf{p})$, where the optimum parameter vector $\mathbf{p}_o$ is obtained by mapping the training image texture and shape into the eigenspace model and the components of $\Delta\mathbf{p}$ are randomly drawn from uniform distributions from -1 to +1 standard deviation.

IV. EXPERIMENTS

A. Setup

Experiments were conducted on 10 knee images manually annotated by a medical expert (Fig. 1). Following the AAM training scheme, a set of different images and corresponding parameter displacements were obtained by randomly perturbing the AAM modes in the interval -1 to +1 standard deviation. While the calculation of $\mathbf{R}$ by numerical differentiation requires separate variation of each AAM mode, CCA-AAM training allows simultaneous variation of all modes. To compare the performance in both cases, AAM segmentation based model was performed on the test data using varying lengths of steps.

B. Faster Training

In Fig. 1, the mean landmark error (point to point distance) over the corresponding number of overall search steps until convergence is depicted. A full rank 10 (bones), CCA employed ranks of 9. It can be observed that the CCA convergence speed with almost equal final accuracy is considerably better than the one of the traditional AAM. The time for an iteration is dominated by the warping in each of the texture comparison steps.

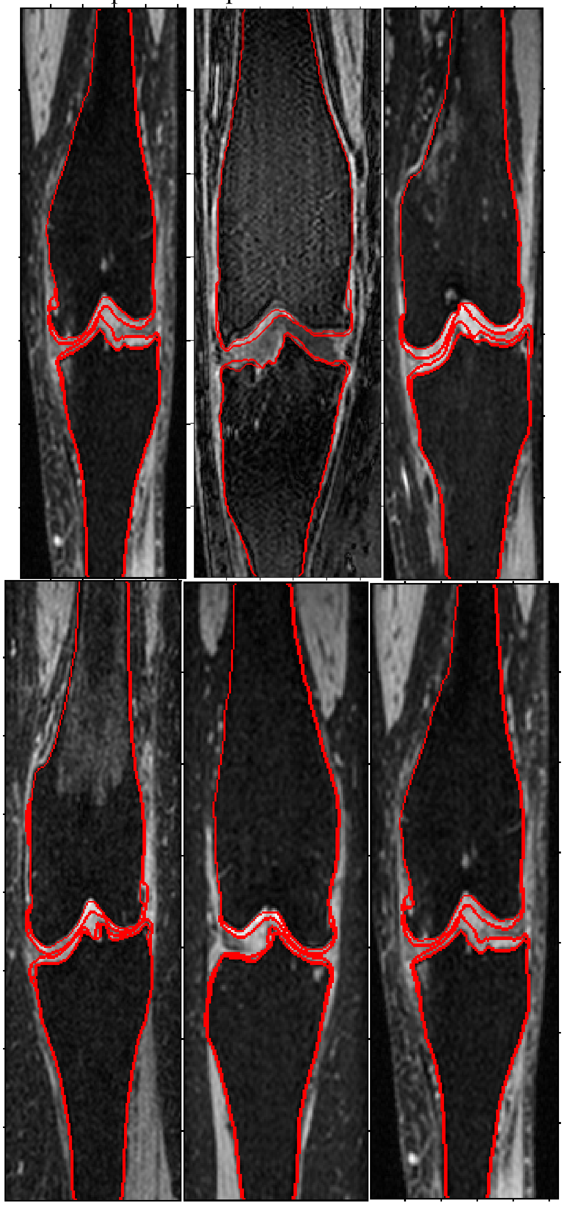

Figure 1. Segmentation results using AAM model.

V. CONCLUSION

CCA-AAMs introduce a search algorithm based on canonical correlation analysis (CCA). CCA efficiently models the dependencies between image residuals and parameter correction. Taking advantage of the correlations between these two signal spaces, CCA makes sensible rank reduction possible. It accounts for noise in the training data and thereby yields significant improvements of the AAM search performance in comparison to the standard search approach. After computing CCA, linear regression is performed on a small number of linear features which leads to a more accurate parameter prediction during search, eliminating the need for the expensive variable step size search scheme employed in the standard approach. Empirical evaluation on two data sets shows that the CCA-AAM search approach is up to four times faster than the standard approach. As fewer training samples are needed, training is up to five times faster.

REFERENCES

[1] T. Cootes and P. Kittipanya-ngam, "Comparing Variations on the Active Appearance Model Algorithm," Proc. British Machine Vision Conf., vol. 2, pp. 837-846, 2002.

[2] T. F. Cootes, G. J. Edwards, and C. J. Taylor, "Active Appearance Models,"Proc. European Conf. Computer Vision (ECCV), pp. 484-498, 1998. citeseer.nj.nec.com/cootes98active.html.

[3] T. Cootes, G. Edwards, and C. Taylor, "A Comperative Evaluation of Active Appearance Model Algorithms," Proc. British Machine Vision Conf., vol. 2, pp. 680-689, 1998.

[4] T. F. Cootes, G. J. Edwards, and C. J. Taylor, "Active Appearance Models," IEEE Trans. Pattern Analysis and Machine Intelligence, vol. 23, no. 6, pp. 681-685, June 2001, citeseer.nj.nec. com/cootes98active.html.

[5] X. Hou, S. Li, H. Zhang, and Q. Cheng, "Direct Appearance Models," Proc. Computer Vision and Pattern Recognition Conf., vol. 1, pp. 828-833, 2001.

[6] I. Matthews and S. Baker, "Active Appearance Models Revisited," Int'l J. Computer Vision, vol. 60, no. 2, pp. 135-164, Nov. 2004.

[7] T. Melzer, M. Reiter, and H. Bischof, "Appearance Models Based on Kernel Canonical Correlation Analysis," Pattern Recognition, vol. 39, no. 9, pp. 1961-1973, 2003.

[8] S. C. Mitchell, J. G. Bosch, B. P. F. Lelieveldt, R. J. van der Geest, J. H. C. Reiber, and M. Sonka, "3-D Active Appearance Models: Segmentation of Cardiac MR and Ultrasound Images," IEEE Trans. Medical Imaging, vol. 21, no. 9, pp. 1167-1178, 2002.

[9] T. Heimann and H-P. Meinzer. Statistical shape models for 3d medical image segmentation: A review. Medical Image Analysis, vol. 13, no. 4, pp. 543- 563, 2009.

[10] T. G. Williams, A. Holmes, J. C. Waterton, R. A. Maciewicz, A. F. P. Nash, and C. J. Taylor. Regional quantitative analysis of knee cartilage in a population study using mri and model based correspondences. ISBI, pp. 11–314, 2006.